Wave dissipation by flexible vegetation

Kassi C. Riffe,[1] Stephen M. Henderson,[1] and Julia C. Mullarney[2]

Received 6 July 2011; revised 18 August 2011; accepted 19 August 2011; published 28 September 2011.

[1] Dissipation of waves propagating through natural salt marsh vegetation was about half the dissipation expected for rigid vegetation. This low dissipation was predicted by a theoretical model that accounts for bending of vegetation motions. A transect of 3 pulse-coherent Acoustic Doppler Profilers recorded water velocity and pressure (at 8 Hz) within the dense (650 stems/m^2) canopy of semi-flexible single-stem vegetation (*Schoenoplectus americanus*). Most wave energy (56–81%) was dissipated within 19 m of the marsh edge. Two dissipation models, the first assuming rigid vegetation, and the second simulating wave-forced vegetation motion using the theory for bending of linearly-elastic beams, were tested. After choosing optimal drag coefficients, both models yielded a good fit to the observed dissipation (skill score = 0.96–0.99). However, fitted drag coefficients for the rigid model (0.58–0.78) were below the range (0.98–2.2) expected for the observed Reynolds numbers (13–450) and canopy densities (accounting for interactions between stem wakes), whereas drag coefficients for the flexible model (0.97–1.6) were nearer the expected range, indicating that prediction of wave dissipation was improved by simulating vegetation motion. **Citation:** Riffe, K. C., S. M. Henderson, and J. C. Mullarney (2011), Wave dissipation by flexible vegetation, *Geophys. Res. Lett.*, *38*, L18607, doi:10.1029/2011GL048773.

1. Introduction

[2] Salt marsh vegetation influences coastal geomorphology [*Hacker and Dethier*, 2006] and promotes sediment deposition [*Kastler and Wiberg*, 1996; *Bartholdy et al.*, 2004] by dissipating waves [*Knutson et al.*, 1982; *Mendez and Losada*, 2004] and currents [*Nepf*, 1999]. Productive saltmarsh ecosystems [*Zedler et al.*, 2001] can retain and remove nutrients [*Gribsholt et al.*, 2007] and pollutants [*Nepf et al.*, 1997; *Gaylord et al.*, 2007].

[3] When vegetation is rigid, wave dissipation can be simulated by calculating drag on individual stems, vertically-integrating the resulting dissipation, and summing over all stems [*Dalrymple et al.*, 1984]. For sufficiently sparse canopies (for sufficiently low λ_p = proportion of bed area occupied by stems), the required depth-variability of velocity can be estimated from frictionless linear wave theory (higher-density canopies, often found very near the bed, can cause leading-order local departures from frictionless theory [*Lowe et al.*, 2005, 2007]). When vegetation is flexible (e.g., giant kelp [*Elwany et al.*, 1995]), wave dissipation is reduced owing to a tendency of stems to move with the surrounding water. This reduced dissipation has been quantified by fitting a rigid vegetation model [*Dalrymple et al.*, 1984] with a reduced effective drag coefficient. Experiments with flexible vegetation [*Bradley and Houser*, 2009; *Kobayashi et al.*, 1993; *Mendez et al.*, 1999; *Mendez and Losada*, 2004; *Augustin et al.*, 2009] show that the fitted effective drag coefficient decreases with increasing Kuelegan-Carpenter number $KC = ut_0/d$ (where u is water velocity, t_0 is wave period and d is stem diameter) and Reynolds number $Re = ud/\nu$ (where ν is kinematic viscosity). However, stem flexibility depends on parameters not included in Re or KC, such as the Young's modulus E. A theoretical model [*Mullarney and Henderson*, 2010] for bending of linearly-elastic stems by linear waves predicts that stem motion and wave dissipation are controlled by a dimensionless stiffness $S = Ed^3t_0/4\rho C_D L^4 u$ (where ρ is water density, C_D is drag coefficient and L is stem length). This theory successfully predicted the observed motion of two intermediate-stiffness stems in a natural saltmarsh. The theory yields previously untested analytic predictions of the increase in wave dissipation with increasing stiffness, from zero dissipation in the fully flexible limit ($S \to 0$) to rapid dissipation in the rigid limit ($S \to \infty$). An alternative theoretical model for dissipation (which represents mobile stems as rigid beams with an elastic hinge at the bed) has been tested in the laboratory [*Mendez et al.*, 1999], but no theoretical model for dissipation by flexible vegetation has previously been tested against field observations of dissipation.

[4] We combine measurements of vegetation geometry and wave attenuation in a natural saltmarsh (Section 2) with a wave energy balance equation (Section 3) to quantify dissipation (Section 4). If standard drag coefficient values are used, then a theoretical model [*Mullarney and Henderson*, 2010] accounting for stem motion predicts wave dissipation more accurately than a rigid-vegetation model [*Dalrymple et al.*, 1984].

2. Field Site and Instrumentation

[5] The field site, located in the marshes of Skagit Bay, Washington (48°21′17.5″ N, 122°28′26.5″ W, Figure 1a), is exposed to short period (~2 s) locally-generated waves, but sheltered from longer period ocean swell. Three bottom-mounted pulse-coherent 2 MHz Nortek Aquadopp Acoustic Doppler Profilers (ADPs) measured wave attenuation along a transect extending 46 m into the marsh (circles, Figure 1a). Each ADP recorded (at 8 Hz) water pressure and vertical profiles of velocity (using 0.04 m bins extending 0.07–0.27 m above the instruments) for a single 256 s burst every 2 hours from 30 July to 14 August 2009. The bed was almost flat, with elevation increasing about 0.04 m from ADP 1 to ADP 3. Mean, rms and maximum along-marsh differences between

[1]School of Earth and Environmental Sciences, Washington State University Vancouver, Vancouver, Washington, USA.
[2]Department of Earth and Ocean Sciences, University of Waikato, Hamilton, New Zealand.

0094-8276/11/2011GL048773

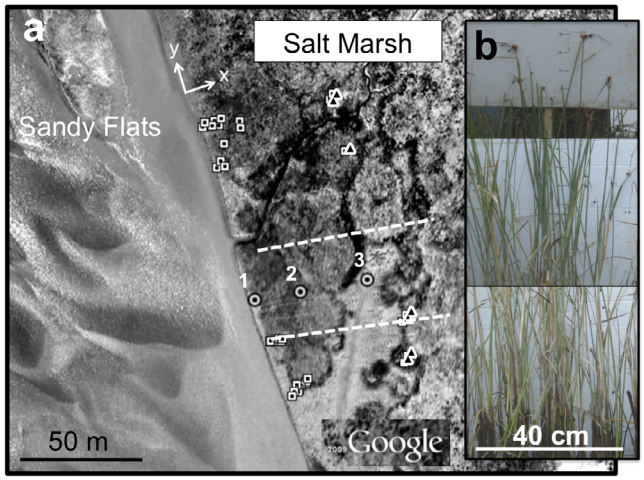

Figure 1. (a) Array of ADPs extending 46 m into the marsh (numbered circles), and vegetation sampling locations (squares and triangles respectively show locations used in calculations of dissipation between instruments 1 & 2 and 2 & 3). Dashed lines mark the bathymetric surveys. Imagery: Google Earth, May 2009. (b) Composite of three close up images of vegetation.

RTK GPS surveys of bed elevation 17 m north and 18 m south of ADP array were respectively 0.03 m, 0.04 m and 0.1 m.

[6] Low correlation ADP data (bins with >50% of correlations in a burst with values <70% on any of the 3 beams) were removed. High frequency wave motions were immeasurably small near the bottom-mounted instruments, partly owing to depth attenuation, so frequencies >0.75 Hz were discarded. Cases with abnormally high acoustic backscatter, or with wave energy flux to pressure variance ratios <67% of unidirectional linear wave theory predictions (likely resulting from seaweed covering instruments) were discarded. The remaining data, though truncated (6% of original data set), represent a range of conditions typical for estuarine salt-marshes: burst-mean depths were h = 0.43–1.2 m, burst-mean currents were $\overline{u}$ = 0–0.09 m/s, and significant wave heights (four times 0.05–0.75 Hz sea-surface standard deviation) were H_s = 0.02–0.12 m.

[7] The single-stem sedge *Schoenoplectus americanus* accounted for >90% of surveyed stems (Figure 1b). Vegetation was surveyed 3 m, 6 m, 9 m and 46 m from the marsh-edge, 20–75 m either side of the ADP array (squares and triangles, Figure 1a). No vegetation samples were collected between ADPs 2 and 3 (Figure 1a, 19 m and 46 m from the marsh edge). At each sample location, the number of stems, the basal diameter, and the height of 12 stems were recorded in a 0.25 m^2 quadrat. Forty quadrats sampled between 14 July 2009 and 14 August 2009 revealed an average height L of 0.8 m, basal diameter d_0 of 5×10^{-3} m, and stem density n of 650 stems/m^2. Caliper measurements [*Mullarney and Henderson*, 2010] and photographs of stem taper (Figure 1b) roughly fitted $d(\zeta)/d_0 = (\zeta/L)^{1/4}$, where $d(\zeta)$ is the stem diameter a distance ζ from the stem-tip [standard deviation of $d(\zeta)/d_0$ at ζ/L = 1/3 was 0.08]. The proportion of bed area occupied by vegetation $\lambda_p = \pi n d^2/4$ ranged from 0.015 to 0.016. For these λ_p values, observations of unidirectional flows (solid curve, Figure 6 of *Nepf* [1999]) suggest that interactions between stem wakes result in a slight (about 12%) reduction in drag.

[8] Burst-averaged Reynolds numbers ranged over Re = 13–450, indicating transitional, rather than fully-turbulent, flow around stems. Kuelegan-Carpenter numbers were KC = 1–91, indicating a transition between oscillatory ($KC \approx 1$) and quasi-steady ($KC \gg 1$) flow. Mean stem length to water depth L/h ranged from 0.8 at high tide to >1 at low tide. Therefore, the observed canopy occupies most or all of the water column, in contrast to the near-bed canopies studied by *Lowe et al.* [2005, 2007], *Bradley and Houser* [2009] and others. Nevertheless, most stem volume was submerged (median 85% and 94% of volume submerged near marsh edge and marsh interior). The median stiffness of measured stems was S = 0.39 (near the marsh edge) and S = 0.62 (near the marsh interior), indicating transitional stiffness. The lower marsh-edge stiffness resulted from the stronger drag exerted by the larger marsh-edge water velocities.

3. Data Analysis

[9] Assuming a statistically steady and along-marsh uniform wave field, the wave energy balance between ADPs located distances x_1 and x_2 from the marsh-edge ($x_2 > x_1$) is [*Mendez and Losada*, 2004]

$$Q_1 - Q_2 = \int_{x_1}^{x_2} \epsilon \, dx, \tag{1}$$

where Q_1 and Q_2 (units of $m^4 s^{-3}$) denote the x component of the wave energy flux at x_1 and x_2, and ε ($m^3 s^{-3}$) is depth integrated dissipation (all energy fluxes, forces and dissipation rates are divided by water density ρ). The decrease in wave energy flux (left of (1), evaluated using ADP data) will be compared with dissipation by vegetation (right of (1), evaluated using models for vegetation drag).

[10] To evaluate Q, measured pressure and velocity were band-passed between 0.05 and 0.75 Hz and substituted into the linear wave theory estimate

$$Q = \frac{1}{\rho} \int_{-h}^{0} \overline{p(z)u(z)} \, dz, \tag{2}$$

where p is pressure (Pa), u is the x velocity component, z is elevation above the mean sea surface, $\overline{X}$ is the burst-mean value of any variable X, and depth-dependence was estimated at every frequency from linear theory [*Guza and Thornton*, 1980]. Since the across-marsh wave energy flux Q is estimated using the across-marsh velocity u, oblique wave propagation is correctly accounted for.

[11] The time-dependent drag at elevation z on a single stem (stem j), per unit stem length (units $m^3 s^{-2}$), is [*Dalrymple et al.*, 1984]

$$\boldsymbol{\delta}_j(z) = \frac{C_D}{2} d_j(z) \left| \boldsymbol{U}_j(z) \right| \boldsymbol{U}_j(z), \tag{3}$$

where bold face denotes a vector quantity, $d_j(z)$ is the diameter of stem j, $\boldsymbol{U}_j(z) = \boldsymbol{u}(z) - \boldsymbol{v}_j(z)$ is the water velocity relative to stem j, $\boldsymbol{u}(z)$ and $\boldsymbol{v}_j(z)$ are the velocities of water and stem j, and the drag coefficient C_D is order-one. The corresponding wave dissipation rate is $\boldsymbol{\delta}_j(z) \cdot \tilde{\boldsymbol{U}}_j(z)$, where $\boldsymbol{U}(z) = \overline{\boldsymbol{U}}(z) + \tilde{\boldsymbol{U}}(z)$, with $\overline{\boldsymbol{U}}(z)$ and $\tilde{\boldsymbol{U}}(z)$ the low (<0.05 Hz,

including mean) and high (0.05–0.75 Hz) frequency components of velocity. The total wave dissipation, per m^2 of bed, resulting from vegetation drag was estimated as

$$\epsilon = n\int_{-h}^{0}\left\langle\overline{\boldsymbol{\delta}(z)\cdot\widetilde{\boldsymbol{U}}(z)}\right\rangle \mathrm{d}z = \frac{nC_D}{2}\int_{-h}^{0}\left\langle d(z)\overline{|\boldsymbol{U}(z)|\boldsymbol{U}(z)\cdot\widetilde{\boldsymbol{U}}(z)}\right\rangle \mathrm{d}z, \quad (4)$$

where $\langle X\rangle = \frac{1}{N_{\mathrm{meas}}}\sum_{j=1}^{N_{\mathrm{meas}}} X_j$ is a mean over all stems, N_{meas} is the number of measured stems, and depth dependence of C_D is neglected. Dissipation was calculated between ADPs 1 and 2 use all stems measured 3 m, 6 m, and 9 m from the marsh-edge (N_{meas} = 348), whereas dissipation was calculated between ADPs 2 and 3 using all stems measured 46 m from the marsh edge (N_{meas} = 96).

[12] To estimate dissipation, the water velocity relative to the (possibly moving) stems $\boldsymbol{U}(z)$ must be determined (equation (4)). However, it is not feasible to measure the motion of all the stems responsible for wave dissipation (e.g., within a 20 m by 10 m region, with a stem density of 650 stems/m^2, about 130,000 stems play a role in wave dissipation). We used two models to estimate the water velocity relative to the stems. In the first, rigid vegetation model, an effective drag coefficient C_{Dr} was calculated by setting the stem velocity $\boldsymbol{v}_j(z)$ to zero in (4), so that $\boldsymbol{U}_j(z)$ equals the (measured) water velocity relative to the earth $\boldsymbol{u}(z)$. In the second, mobile vegetation model, $\boldsymbol{U}_j(z)$ was simulated along the length of every measured stem using the model of *Mullarney and Henderson* [2010] to simulate stem motion. When stems emerged from the water, stem length was set equal to the depth, an approach that neglects inertia of above-water sections of stems (>85% of stem volume was submerged in most cases, Section 2). Vegetation stiffness was calculated using a Young's modulus $E = 1 \times 10^8$ Pa, previously determined by fitting the straight-stem model of *Mullarney and Henderson* [2010] to the observed motion of two stems (and consistent with direct measurements of E for this species by Tolle and Albert (personal communication, 2010)). For every measured stem (444 stems) and every burst, the model simulated drag, stem deformation and dissipation at all frequencies between 0.05 and 0.75 Hz. Fourier components of water velocity $\boldsymbol{u}$(z) were calculated as a function of elevation using ADP measurements and linear-theory depth-attenuation. Vertical structure was then projected onto the first ten normal modes of the Euler-Bernoulli beam equation [*Mullarney and Henderson*, 2010]. The model was run twice, once with the measured Young's modulus, and once assuming perfectly rigid stems (for narrow-banded Gaussian waves, the rigid-stem limit of the *Mullarney and Henderson* [2010] model reduces to the *Dalrymple et al.* [1984] model). For each burst and instrument location, one value of the ratio r between the total dissipation (summed over all N_{meas} stems for that location) for flexible and rigid vegetation was calculated. Between ADPs 1 and 2 (between ADPs 2 and 3), the mean r over all bursts was 0.53 (0.63) and the standard deviation was 0.070 (0.067). The slightly lower marsh-edge r is consistent with the lower marsh-edge vegetation stiffness (Section 2). The final estimated dissipation rate for the flexible model (for each burst and location) was calculated by multiplying the rigid model's dissipation rate by r.

[13] Modeled dissipation rates at each ADP were interpolated to estimate the across-marsh-integrated dissipation appearing on the right of (1). Integrating (4) between x_1 and x_2 yields (for the rigid model)

$$\int_{x_1}^{x_2}\epsilon \mathrm{d}x = C_{D_r}\mathcal{R}_{1,2} \quad (5)$$

and (for the flexible model)

$$\int_{x_1}^{x_2}\epsilon \mathrm{d}x = C_{D_f}\mathcal{F}_{1,2}, \quad (6)$$

where $\mathcal{R}_{1,2} = \frac{1}{2}\int_{x_1}^{x_2}\int_{-h}^{0} n\langle d(z)\,\overline{|\boldsymbol{U}(z)|\boldsymbol{U}(z)\cdot\tilde{\boldsymbol{U}}(z)}\rangle\,\mathrm{d}z\,\mathrm{d}x$, $\mathcal{F}_{1,2} = r\mathcal{R}_{1,2}$ and across-marsh variation was estimated by fitting the theoretical $(\alpha+\beta x)^{-1}$ dependence of wave amplitude, where α and β are constants [*Mendez and Losada*, 2004].

[14] One value of Q, $\mathcal{R}$ and $\mathcal{F}$ was estimated for every 256 s ADP burst. Velocity measurements were noisier than pressure, leading to unrealistically high measured velocity variances. To prevent this high noise from biasing dissipation estimates, velocities in (4) were estimated by adding the mean current $\bar{u}$, measured by the ADPs, to a synthetic wave-frequency velocity $\tilde{U}$, estimated from pressure using linear theory and a wave direction equal to the direction of the burst-mean energy flux. Instrument noise did not bias Q estimates (because noise in pressure and velocity are uncorrelated), but pressure noise biased $\mathcal{R}$ and $\mathcal{F}$ high by 2–4% (based on noise measured by instruments submerged in a still laboratory tank). Regressing observed $Q_1 - Q_2$ against $\mathcal{R}_{1,2}$ and $\mathcal{F}_{1,2}$ yields C_{Dr} and C_{Df} (1). Similar analysis was applied between ADPs 2 and 3. If vegetation motion were significant and simulated correctly by the flexible model, then the fitted flexible-model drag coefficient C_{Df} would approximate the true drag coefficient. In contrast, the fitted rigid-model drag coefficient C_{Dr} would have a non-physical low value, to compensate for the neglected reduction in dissipation resulting from vegetation motion.

[15] We have neglected frictional effects when calculating the vertical structure of the velocity from linear wave theory. Theory suggests that this simplification is justified when

$$\lambda_p \ll \min\left[1, \frac{\pi^2}{C_D KC}\right]. \quad (7)$$

Condition (7) is derived by noting that local departures from frictionless wave theory (represented by the second and third terms on the right of equation 22 of *Lowe et al.* [2005, hereinafter (L22)]) become small in the limit (7) (note that Lowe's A_{rms} equals $2\pi dKC$, and the first term on the right of (L22) is zero for emergent canopies). Measurements confirm that condition (7) is satisfied by the vegetation canopies considered here (λ_p did not exceed 0.016, while $\pi^{-2}C_D KC\lambda_p$ never exceeded 0.089 and had median value 0.04 (0.01) near the marsh-edge (marsh interior)). Since (7) is satisfied, leading-order reductions in wave height are expected only after waves have propagated many wavelengths (many meters).

4. Results and Discussion

[16] Rapid wave dissipation was observed, with the wave energy flux decreasing by 56–81% in the 19 m between the two instruments nearest the marsh-edge (ADPs 1 and 2 of Figure 1a). This dissipation exceeded the dissipation

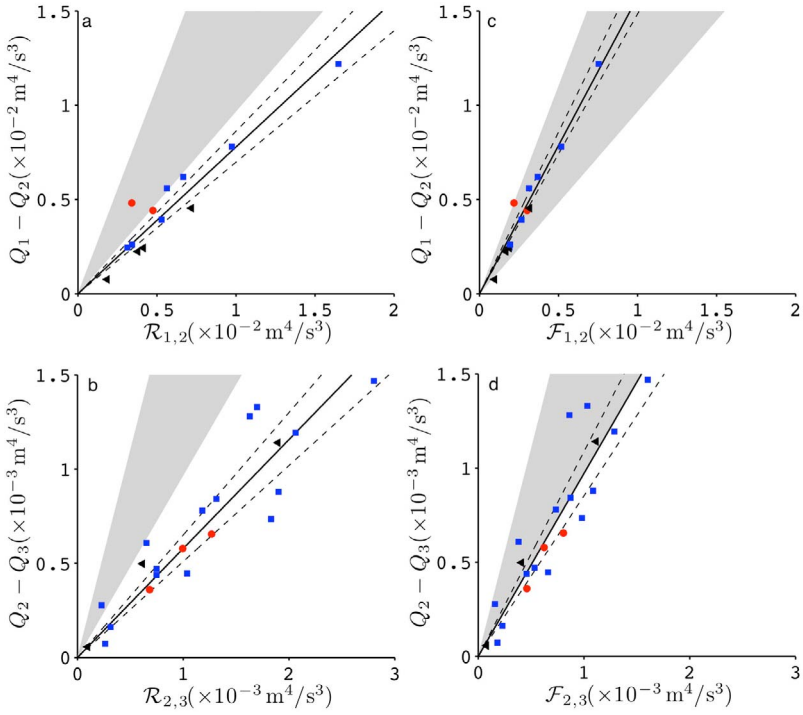

Figure 2. Change in energy flux between (a, c) instruments 1 & 2, and (b, d) instruments 2 & 3 versus dissipation predicted by models for rigid vegetation (Figures 2a and 2b) and flexible vegetation (Figures 2c and 2d). Horizontal axes were normalized so that slope equals drag coefficient (equations (5) and (6)). Triangles, squares and circles respectively represent ~256 s averages for which $L/h < 0.8$, $0.8 < L/h < 1.2$ and $L/h > 1.2$, where L = mean stem length, h = water depth. Grey shaded regions indicate $C_D = 0.98 - 2.2$, the range expected for the observed Reynolds numbers and vegetation densities when accounting for wake-interaction effects. Dashed lines show 95% confidence intervals on the fitted drag.

associated with bottom friction by 2800% (assuming an upper-bound bottom drag coefficient of $f_e = 0.2$, [*Tolman*, 1994]), indicating that vegetation drag dominated dissipation. Pressure-velocity co-spectra (not shown) revealed that 0.3–0.8 Hz waves usually dominated the wave energy flux.

[17] After fitting the drag coefficient C_{Dr}, the skill score for the rigid model, applied to all m bursts,

$$\text{skill score} = 1 - \frac{\sum_{i=1}^{m}\left[\left(Q_1 - Q_2 - C_{D_r}\mathcal{R}_{1,2}\right)^2\right]_i}{\sum_{i=1}^{m}\left[\left(Q_1 - Q_2\right)^2\right]_i} \qquad (8)$$

(where $_i$ denotes value for burst i) was 0.97 between ADPs 1 and 2 ($m = 13$), and 0.96 between ADPs 2 and 3 ($m = 21$), indicating a strong linear relationship between rigid-model predictions and observations (Figures 2a and 2b). However, fitted rigid-model drag coefficients were $C_{Dr} = 0.78$ (ADPs 1–2) and 0.58 (ADPs 2–3), below the range expected at the observed Reynolds numbers, even after the estimated effect of wake interactions is accounted for. For steady flow around isolated cylinders $C_D = 1.1$–2.5 for $Re = 450$–13 [*Clift et al.*, 1978, equations 6.20–6.22]. Similar values are measured around randomly-oriented beams with triangular cross-section [*Cheng and Liu*, 2000], suggesting that deviations from circular cross-sections are unlikely to explain the low C_{Dr} values. Time variability can not explain low C_{Dr} values, because C_D approximates steady-flow values at high KC, and rises above steady values as KC drops below about 20 [*Sarpkaya*, 1986; *Zhou and Graham*, 2000]. Accounting for interactions between stem wakes (Section 2) reduces the expected range to $C_D = 0.98 - 2.2$. No dependence of drag coefficient on stem length-to-depth ratio was evident (compare triangles, diamonds, and circles of Figures 2a and 2b).

[18] The flexible-vegetation model yielded skill scores of 0.99 (ADPs 1–2) and 0.96 (ADPs 2–3), with corresponding fitted drag coefficients $C_{Df} = 1.6$ and 0.97 (Figures 2c and 2d). These drag coefficients exceed rigid-model values (C_{Dr}) by 170–200%, indicating that the flexible-stem model predicted substantially reduced dissipation owing to stem motion. Between ADPs 1 and 2, the fitted flexible-stem drag coefficient was within the range expected given the observed Re. Between ADPs 2 and 3, the fitted flexible-stem coefficient, although higher than the rigid coefficient, was still slightly (13%) below the expected range when possible wake interactions are neglected. However, correction for wake interactions brings the fitted coefficient within 1% of the expected range $C_D = 0.98 - 2.2$ (compare grey regions with solid lines, Figures 2c and 2d). No dependence of drag coefficient on stem length-to-depth ratio was evident (compare triangles, squares and circles of Figures 2c and 2d).

[19] The scatter of data plotted in Figure 2 introduces some uncertainty to C_D estimates. Further uncertainty, resulting from vegetation sampling (which does not contribute scatter to Figure 2 because the same surveys were

used for all bursts), was estimated from the standard deviation of nd_0 (to which fitted C_D is roughly inversely proportional, equation (4)). Unresolved spatial variations in vegetation properties (no samples were collected between ADPs 2 and 3, see Section 2) may cause errors to exceed this estimate. Treating the errors in C_D estimates arising from scatter and from vegetation sampling as independent, 95% confidence intervals for the rigid model were C_{Dr} = 0.70 − 0.86 (ADPs 1–2), and C_{Dr} = 0.51 − 0.65 (ADPs 2–3). Corresponding 95% confidence intervals for the flexible model were C_{Df} = 1.48 − 1.72 (ADPs 1–2) and C_{Df} = 0.85 − 1.09 (ADPs 2–3). All estimated drag coefficients are biased low by a further 2–4% owing to noise in pressure measurements (Section 3). In all cases, confidence intervals for drag coefficients estimated using the flexible model overlap the expected range, whereas intervals for coefficients estimated using the rigid model do not (compare dashed lines and grey regions, Figure 2).

5. Conclusions

[20] Using hydrodynamic data and vegetation surveys in a natural salt marsh, we have tested models for wave dissipation by vegetation. If standard drag coefficients are used, a rigid-vegetation model underpredicts wave dissipation by about a factor of 2. Higher accuracy is achieved (using standard drag coefficients) by a theoretical model that accounts for vegetation motion.

[21] These results indicate that vegetation motion substantially reduced wave dissipation. Similar reductions in dissipation have been observed previously, but simulation of the motion of many stems in a natural canopy has not previously been attempted. The model used here approximately predicted the observed reduction in dissipation without tuning (the potential tuning parameter, Young's modulus, was not modified from the value previously chosen by *Mullarney and Henderson* [2010] to fit observed motion of two stems). This suggests that analytic models can, at least for certain vegetation types, provide useful predictions of wave dissipation by natural flexible canopies.

[22] **Acknowledgments.** Funding was provided by the Office of Naval Research and State of Washington. Tammy Lee, Kara Goodwin, Chris Eager, Chris Scheffler, Nate Raynor and Lisa Hodges assisted with vegetation surveys, instrument deployment and maintenance. We thank the anonymous reviewers for their helpful comments.

[23] The Editor thanks two anonymous reviewers for their assistance in evaluating this paper.

References

Augustin, L., J. Irish, and P. Lynett (2009), Laboratory and numerical studies of wave damping by emergent and near-emergent wetland vegetation, *Coastal Eng.*, *56*, 332–340.

Bartholdy, J., C. Christiansen, and H. Kunzendorf (2004), Long term variations in backbarrier salt marsh deposition on the Skallingen peninsula —The Danish Wadden Sea, *Mar. Geol.*, *203*, 1–21.

Bradley, K., and C. Houser (2009), Relative velocity of seagrass blades: Implications for wave attenuation in low-energy environments, *J. Geophys. Res.*, *114*, F01004, doi:10.1029/2007JF000951.

Cheng, M., and G. Liu (2000), Effects of afterbody shape on flow around prismatic cylinders, *J. Wind Eng. Ind. Aerodyn.*, *84*, 181–196.

Clift, R., J. Grace, and M. Weber (1978), *Bubbles, Drops and Particles*, Dover, Mineola, N. Y.

Dalrymple, R., J. Kirby, and P. Hwang (1984), Wave diffraction due to areas of energy dissipation, *J. Waterw. Port Coastal Ocean Eng.*, *110*(1), 67–79.

Elwany, M., W. O'Reilly, R. Guza, and R. Flick (1995), Effects of Southern California kelp beds on waves, *J. Waterw. Port Coastal Ocean Eng.*, *121*(2), 143–150.

Gaylord, B., et al. (2007), Spatial patterns of flow and their modification within and around a giant kelp forest, *Limnol. Oceanogr.*, *52*(5), 1838–1852.

Gribsholt, B., et al. (2007), Nitrogen assimilation and short term retention in a nutrient-rich tidal freshwater marsh—A whole ecosystem ^{15}N enrichment study, *Biogeosciences*, *4*, 11–16.

Guza, R. T., and E. B. Thornton (1980), Local and shoaled comparisons of sea surface elevations, pressures, and velocities, *J. Geophys. Res.*, *85*, 1524–1530.

Hacker, S. D., and M. N. Dethier (2006), Community modification by a grass invader has differing impacts for marine habitats, *Oikos*, *113*(2), 279–286.

Kastler, J. A., and P. L. Wiberg (1996), Sedimentation and boundary changes of Virginia salt marshes, *Estuarine Coastal Shelf Sci.*, *42*, 683–700.

Knutson, P. L., R. a. Brochu, W. N. Seelig, and M. Inskeep (1982), Wave damping in *Spartina alterniflora* marshes, *Wetlands*, *2*, 87–104.

Kobayashi, N., A. Raichle, and T. Asano (1993), Wave attenuation by vegetation, *J. Waterw. Port Coastal Ocean Eng.*, *119*(1), 30–48.

Lowe, R. J., J. R. Koseff, and S. G. Monismith (2005), Oscillatory flow through submerged canopies: 1. Velocity structure, *J. Geophys. Res.*, *110*, C10016, doi:10.1029/2004JC002788.

Lowe, R. J., J. L. Falter, J. R. Koseff, S. G. Monismith, and M. J. Atkinson (2007), Spectral wave flow attenuation within submerged canopies: Implications for wave energy dissipation, *J. Geophys. Res.*, *112*, C05018, doi:10.1029/2006JC003605.

Mendez, F. J., and I. J. Losada (2004), An empirical model to estimate the propagation of random breaking and nonbreaking waves over vegetation fields, *Coastal Eng.*, *51*, 103–118.

Mendez, F. J., I. J. Losada, and M. A. Losada (1999), Hydrodynamics induced by wind waves in a vegetation field, *J. Geophys. Res.*, *104*, 18,383–18,396.

Mullarney, J. C., and S. M. Henderson (2010), Wave-forced motion of submerged single-stem vegetation, *J. Geophys. Res.*, *115*, C12061, doi:10.1029/2010JC006448.

Nepf, H. M. (1999), Drag, turbulence, and diffusion in flow through emergent vegetation, *Water Resour. Res.*, *35*, 479–489.

Nepf, H., C. Mugnier, and R. Zavistoski (1997), The effects of vegetation on longitudinal dispersion, *Estuarine Coastal Shelf Sci.*, *44*, 675–684.

Sarpkaya, T. (1986), Force on a circular cylinder in viscous oscillatory flow at low Keulegan-Carpenter numbers, *J. Fluid Mech.*, *165*, 61–71.

Tolman, H. L. (1994), Wind waves and moveable-bed bottom friction, *J. Phys. Oceanogr.*, *24*, 994–1009.

Zedler, J., J. Callaway, and G. Sullivan (2001), Declining biodiversity: Why species matter and how their functions might be restored in Californian tidal marshes, *BioScience*, *51*(12), 1005–1017.

Zhou, C., and J. Graham (2000), A numerical study of cylinders in waves and currents, *J. Fluids Struct.*, *14*, 403–428.

S. M. Henderson and K. C. Riffe, School of Earth and Environmental Sciences, Washington State University Vancouver, 14204 NE Salmon Creek Ave., Vancouver, WA 98686, USA. (reedie4life@gmail.com)

J. C. Mullarney, Department of Earth and Ocean Sciences, University of Waikato, Private Bag 3105, Hamilton 3240, New Zealand.